

# Realization of High-NOON States by Mixing Quantum and Classical Light

Itai Afek, Oron Ambar, Yaron Silberberg\*

Department of Physics of Complex Systems, Weizmann Institute of Science,  
Rehovot 76100, Israel

\* E-mail: yaron.silberberg@weizmann.ac.il

**Precision measurements can be brought to their ultimate limit by harnessing the principles of quantum mechanics. Particularly useful, to this end, are multi-particle entangled states of the ‘Schrödinger cat’ type, known as NOON states. In optics, photonic NOON states can be used to obtain high precision phase measurements, becoming more and more advantageous as the number of photons grows. Here, we generate ‘high-NOON’ states by multiphoton interference of ‘quantum’ down-converted light with a ‘classical’ coherent state. Super-resolving phase measurements with up to five entangled photons are demonstrated with a visibility higher than obtainable without entanglement. The approach is inherently scalable to arbitrarily high photon numbers, with immediate implications to all areas of quantum measurement.**

Entanglement is a distinctive feature of quantum mechanics which lies at the core of many new applications in the emerging science of quantum information. Multi-particle entangled states are central to quantum computing, teleportation and quantum metrology (*1*). A particularly useful class of states are the maximally path entangled NOON states,

$|N :: 0\rangle_{a,b} \equiv \frac{1}{\sqrt{2}} (|N, 0\rangle_{a,b} + |0, N\rangle_{a,b})$ , which contain  $N$  indistinguishable particles in an equal superposition of all being in one of two possible paths  $a$  and  $b$  (2). These states are ‘Schrödinger cats’ since they consist of a superposition of two highly distinct states corresponding to the ‘dead’ and ‘alive’ cat. The larger the value of  $N$  the bigger the cat is; thus bringing us closer to the regime of macroscopic entanglement envisioned originally by Schrödinger (3). Realization of such states is required for the experimental study of fundamental questions such as the effect of decoherence on many particle entanglement (4, 5). In addition, NOON states are the enabling technology behind various quantum measurement schemes. In optics, a NOON state with  $N$  entangled photons acquires a phase at a rate  $N$  times faster than classical light (6). This leads to enhanced phase sensitivity, which can be used for reaching the fundamental Heisenberg limit (2), and to phase super-resolution which is the key to sub-Rayleigh resolution in quantum lithography (7).

Our goal is to generate optical NOON states with high photon numbers. Various schemes for generating such states have been suggested (2, 8–13). However, the three photon record of leading experiments (14, 15) has proven difficult to surpass. We note that a ‘NOON-like’ four photon state has been generated, but only by using four rather than two spatial modes (16). In addition, a number of experiments have used state projection to focus on the NOON component of various initial  $N$  photon states (16–19).

Here, we show the first experimental realization of an approach introduced by Hofmann and Ono (20), which yields NOON states with arbitrarily high photon numbers. The underlying principle is that when a ‘classical’ coherent state and ‘quantum’ down-converted light are mixed properly using a standard beamsplitter (BS), the emerging state shows ‘Schrödinger cat’ like behavior, i.e. all the photons exit from one of the BS ports or the other (Fig. 1A). The approach is appealing due to its inherent simplicity relying on a fundamental unmodified multiphoton interference effect. Consider a 50/50 beam-splitter fed by a coherent state,  $|\alpha\rangle_a$ , in one input

port and spontaneous parametric down-conversion (SPDC),  $|\xi\rangle_b$ , in the other (see Fig. 2A). The input states are defined in the conventional way (6)

$$\begin{aligned} |\alpha\rangle &= \sum_{n=0}^{\infty} e^{-\frac{1}{2}|\alpha|^2} \frac{\alpha^n}{\sqrt{n!}} |n\rangle, \quad \alpha = |\alpha|e^{i\phi_{cs}} \\ |\xi\rangle &= \frac{1}{\sqrt{\cosh r}} \sum_{m=0}^{\infty} (-1)^m \frac{\sqrt{(2m)!}}{2^m m!} \\ &\quad \times (\tanh r)^m |2m\rangle, \end{aligned} \quad (1)$$

where the phase of  $|\xi\rangle$  has been set arbitrarily to zero leaving the relative phase of the two inputs to be determined by  $\phi_{cs}$ . We denote the pair amplitude ratio of the coherent state and SPDC inputs by  $\gamma = |\alpha|^2/r$ . In physical terms  $\gamma^2$  is the two photon probability of the classical source divided by that of the quantum source. The larger the value of  $\gamma$ , the higher the relative weight of the classical resources. The state at the BS output,  $|\psi_{out}\rangle_{c,d}$ , is highly path entangled. A general  $N$  photon two-mode state can be written as  $\sum_{k=0}^N u_k |k\rangle_c |N-k\rangle_d$ . The creation of an ideal NOON state would require elimination of all the ‘non-NOON’ components i.e.  $u_1, \dots, u_{N-1} = 0$ . Remarkably, the present scheme does this almost perfectly using the naturally emerging multiphoton interference (Fig. 1A). The fidelity of the output state’s normalized  $N$  photon component with a NOON state is  $F_N \equiv |\langle N :: 0 | \psi_{out}^N \rangle|^2$ . It can be shown that by choosing  $\phi_{cs} = \pi/2$  and optimizing  $\gamma$  for each  $N$ , one can achieve  $F_N > 0.92$  for arbitrary  $N$ , see Fig. 1C. The theoretical overlaps for the states generated in this work are  $F_N = 1, 1, 0.933, 0.941$  for  $N = 2, 3, 4, 5$  respectively. We note that the four photon value is much higher than the theoretical fidelity of 0.75 obtainable using down-conversion only (19, 21).

To verify the  $N$ -photon coherence of the generated states we employ a Mach-Zehnder interferometer, see Fig. 2. This is the prototypical setup used in schemes for quantum lithography and reduced noise interferometry (2). The quantum and classical inputs are prepared in perpendicular linear polarizations ( $H, V$ ) and spatially overlapped using a polarizing beam-splitter (PBS). A Mach-Zehnder interferometer (MZ) is then implemented in an inherently

phase stable, collinear design so that the NOON state mode subscripts  $c, d$  may now be replaced by  $X, Y$  ( $\pm 45$  deg. polarizations). After application of the MZ phase shift  $\varphi$ , the state  $|N0\rangle_{X,Y} + |0N\rangle_{X,Y}$  evolves to  $|N0\rangle_{X,Y} + e^{iN\varphi}|0N\rangle_{X,Y}$  (2). This gives rise to interference oscillations  $N$  times faster than those of a single photon with the same frequency.

The experimental results are shown in Fig. 3. Two to five photon coincidence rates were measured as a function of the MZ phase. We denote the number of photon 'clicks' in  $D_1(D_2)$  by  $N_1(N_2)$ . The  $N_1, N_2$  coincidence rate is expected to demonstrate a de-Broglie wavelength (6) of  $\lambda/N$ , where  $N = N_1 + N_2$  is the total number of photons. The red curves are produced by an analytical model of the experiment, accounting for the overall transmission and the positive operator-value measures (POVM) of the detectors (see supporting online text). The two and three photon results were measured simultaneously with  $\gamma_2 = \gamma_3 = 1$  (the subscript of  $\gamma$  denotes the value of  $N$  for which it was optimized). For this measurement we used a mere 2mW of ultraviolet power to pump the SPDC. The results in Figs. 3C-D constitute the highest visibility measurement of a three photon NOON state to date (14, 15) ( $86 \pm 0.6\%$  for 2, 1 and  $80 \pm 1.9\%$  for 3, 0). The four photon measurements were taken with  $\gamma_4 = \sqrt{3}$  and using 25mW of ultraviolet pump. They exhibit similar visibilities for both the 3, 1 ( $74 \pm 3\%$ ) and the 2, 2 ( $73 \pm 2.4\%$ ) options. Finally, the  $N = 5$  result is, to the best of our knowledge, the first realization of a five photon NOON state ( $V = 42 \pm 2\%$  for 3, 2). This measurement was taken using 215mW of ultraviolet pump and setting  $\gamma_5 = 9/(\sqrt{10} + 1) \sim 2.16$  implying that ( $\gamma_5^2 \sim$ )4.7 times more photon pairs originate from the coherent state than from the SPDC. All the above visibilities manifest the high NOON state overlap of the generated states. These visibilities significantly exceed the super-resolution bound for classical states which we have recently derived (22). In particular the classical bound for the five photon measurement is 16.67% which we have surpassed by more than 12 standard deviations.

The visibility of the experimental plots in Fig. 3 is determined by the overall setup trans-

mission which we denote  $\eta$ . For  $\eta < 1$ , high order events contribute a background to the  $N$ -fold coincidence rate. In the current setup we estimate  $\eta \sim 0.12$  based on the SPDC coincidence to singles ratio. We note that reasonable improvement of the transmission could allow generating states even larger than currently demonstrated (see supporting online text for details).

It is interesting, that the  $N$ -fold coincidence plots of Fig. 1D exhibit  $N$  zero points as expected by perfect maximally path entangled states albeit with somewhat modulated peak heights. In fact, it has been shown (20) that due to the high fidelity we can expect a phase sensitivity that is only slightly lower than the Heisenberg limit for a given  $N$  photon component. Thus, the small deviation from an ideal NOON state is not a major limiting factor and is more than compensated for by the intrinsic 100% efficiency. Furthermore, while the state at hand is optimized for a given  $N = N_0$ , there is a range of  $N$  values surrounding  $N_0$  which also have considerable NOON fidelity (Fig 2A,C). Thus, the generated state is actually a superposition of NOON states with various photon numbers, each of which contributes to the enhanced phase sensitivity. As a result, the current method allows beating the standard quantum limit both for specific  $N$  (19) and while accounting for the complete photon number distribution (23).

The realized scheme has several unique properties (20). Most importantly, it works naturally for arbitrary  $N$ . This requires no alterations to the setup except for use of detectors which can resolve  $N$  photon events and setting  $\gamma$  appropriately. This is in contrast to previous experiments which were customized to a specific value of  $N$  (14, 15, 24). In addition, most of the photons in this scheme originate from the coherent (classical) light source which is practically unlimited in intensity. This eliminates the need for bright SPDC sources, providing a significant experimental simplification. Finally, the scheme involves no state projection or post selection, implying that all the  $N$ -photon events contribute to the measurable  $N$ -photon interferences.

It is interesting, that a setup very similar to the one in Fig. 2A, yet with much stronger light fields, is commonly used for obtaining quantum noise reduction using homodyne detection

(6). Homodyne detection is a highly developed technique, based on the measurement of the continuous variable field quadratures. Our experiment demonstrates that extending the concept of squeezed vacuum and coherent light interference into the weak local oscillator regime is extremely fruitful. The states emerging from this interference, for a given  $N$ , are almost perfect NOON states. This implies a fundamental connection between quantum noise reduction (with continuous variables) and creation of NOON states (in photon-number resolving experiments).

To summarize, super-resolving phase measurements beyond the classical limit have been demonstrated with up to five entangled photons. This is the highest order of super-resolution obtained to date in a setup compatible with the original quantum lithography proposal (7). Rather than requiring more non-classical resources, the key to extending this work to even higher NOON states is in improving the overall transmission. This highlights the need for high purity SPDC sources which can be spectrally mode matched to coherent states (25–27). Improved single mode coupling of the photon pairs and high efficiency photon number resolving detectors (28, 29) would also be extremely beneficial. The inherent scalability we have demonstrated opens the way to exciting applications in high sensitivity interferometry, quantum imaging and sub-Rayleigh lithography.

## References

1. M. Nielsen, I. Chuang, *Quantum Computation and Quantum Information* (Cambridge University Press, Cambridge, 2000).
2. J. Dowling, *Contemp. Phys.* **49**, 125 (2008).
3. E. Schrödinger, *Naturwissenschaften* **23**, 807 (1935).
4. L. Aolita, R. Chaves, D. Cavalcanti, A. Acín, L. Davidovich, *Phys. Rev. Lett.* **100**, 080501 (2008).

5. H. S. Eisenberg, G. Khoury, G. A. Durkin, C. Simon, D. Bouwmeester, *Phys. Rev. Lett.* **93**, 193901 (2004).
6. C. C. Gerry, P. L. Knight, *Introductory Quantum Optics* (Cambridge University Press, 2005).
7. A. N. Boto, *et al.*, *Phys. Rev. Lett.* **85**, 2733 (2000).
8. K. T. McCusker, P. G. Kwiat, *Phys. Rev. Lett.* **103**, 163602 (2009).
9. K. T. Kapale, J. P. Dowling, *Phys. Rev. Lett.* **99**, 053602 (2007).
10. H. Cable, J. P. Dowling, *Phys. Rev. Lett.* **99**, 163604 (2007).
11. G. J. Pryde, A. G. White, *Phys. Rev. A* **68**, 052315 (2003).
12. J. Fiurášek, *Phys. Rev. A* **65**, 053818 (2002).
13. H. F. Hofmann, *Phys. Rev. A* **70**, 023812 (2004).
14. M. W. Mitchell, J. S. Lundeen, A. M. Steinberg, *Nature* **429**, 161 (2004).
15. H. Kim, H. S. Park, S.-K. Choi, *Opt. Express* **17**, 19720 (2009).
16. P. Walther, *et al.*, *Nature* **429**, 158 (2004).
17. B. H. Liu, *et al.*, *Phys. Rev. A* **77**, 023815 (2008).
18. K. J. Resch, *et al.*, *Phys. Rev. Lett.* **98**, 223601 (2007).
19. R. Okamoto, *et al.*, *New J. Phys.* **10**, 073033 (2008).
20. H. F. Hofmann, T. Ono, *Phys. Rev. A* **76**, 031806 (2007).
21. T. Nagata, R. Okamoto, J. L. O'Brien, K. Sasaki, S. Takeuchi, *Science* **316**, 726 (2007).

22. I. Afek, O. Ambar, Y. Silberberg, *ArXiv e-prints* 1002.0684v1.
23. L. Pezzé, A. Smerzi, *Phys. Rev. Lett.* **100**, 073601 (2008).
24. Y. J. Lu, Z. Y. Ou, *Phys. Rev. Lett.* **88**, 023601 (2001).
25. P. J. Mosley, *et al.*, *Phys. Rev. Lett.* **100**, 133601 (2008).
26. P. J. Mosley, J. S. Lundeen, B. J. Smith, I. A. Walmsley, *New J. Phys.* **10**, 093011 (2008).
27. A. Valencia, A. Ceré, X. Shi, G. Molina-Terriza, J. P. Torres, *Phys. Rev. Lett.* **99**, 243601 (2007).
28. C. Silberhorn, *Contemp. Phys.* **48**, 143 .
29. A. E. Lita, A. J. Miller, S. W. Nam, *Opt. Express* **16**, 3032 (2008).
30. We thank Barak Dayan for helpful discussions. Itai Afek gratefully acknowledges the support of the Ilan Ramon Fellowship. Financial support of this research by the German Israeli foundation is gratefully acknowledged.

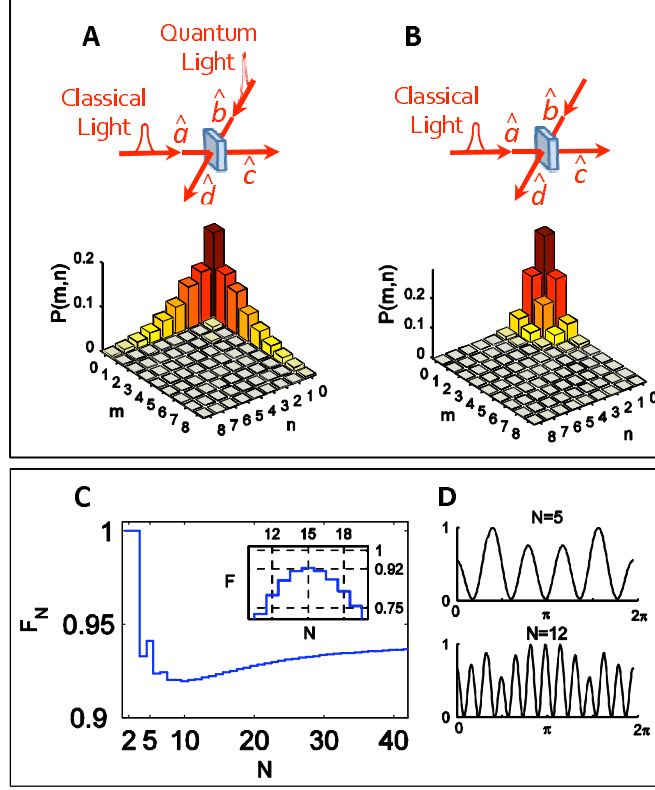


Figure 1: Theoretical properties of the generated states. **A**, Classical light is mixed with ‘quantum’ SPDC light on a beamsplitter. Bar heights represent the probability for  $m, n$  photons in output modes  $c, d$  respectively. The ‘corner’-like shape illustrates the tendency of all the photons to collectively exit from the same output port, exhibiting ‘Schrödinger cat’ like behavior. The average flux is 1.2 photons per pulse from each input. **B**, The same as **A** but using only classical light; shown for comparison. The photons at the outputs are clearly in a separable (unentangled) state. **C**, Fidelity,  $F_N$  vs.  $N$  in an ideal setup. The pair amplitude ratio  $\gamma$ , which maximizes the NOON state overlap was chosen separately for each  $N$ . Optimal fidelity is always larger than 0.92, and it approaches 0.943 asymptotically for large  $N$ . The inset shows that when  $\gamma$  is optimized for  $N = 15$ , the fidelity for nearby  $N$  is also high. In this case  $F > 0.75$  for  $N = 12$  to 19, simultaneously. **D**, Simulated  $N$ -fold coincidences as a function of Mach-Zehnder phase for  $N = 5, 12$  demonstrating  $N$ -fold super-resolution.

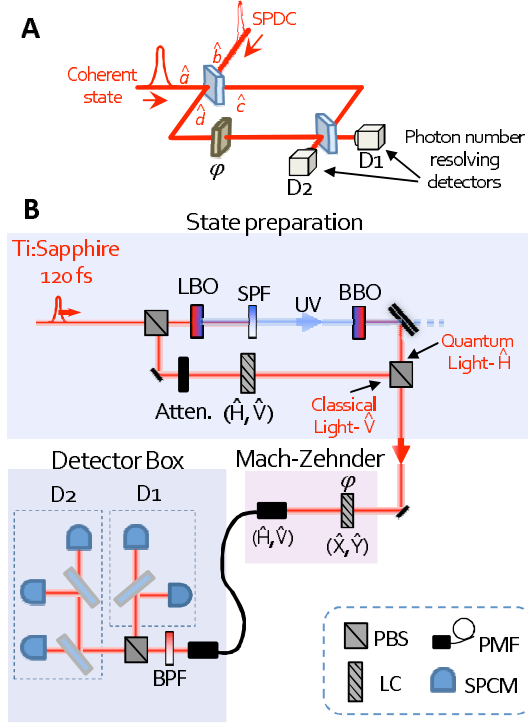


Figure 2: Experimental Setup. **A**, Schematic of the setup depicting a Mach-Zehnder (MZ) interferometer fed by a coherent state and SPDC. The NOON states occur in modes  $c$  and  $d$  after the first beamsplitter. Measurement of multi-photon coincidences is performed using photon number resolving detectors. **B**, Detailed layout of the setup. A pulsed Ti:Sapphire oscillator with 120 fs pulses @80 MHz is doubled using a 2.74mm LBO crystal to obtain 404nm ultra-violet pulses with maximum power of 225mW. These pulses then pump collinear degenerate type-I SPDC @808nm using a 1.78mm BBO crystal. The SPDC (H pol.) is mixed with attenuated coherent light (V pol.) using a polarizing beam-splitter (PBS). A thermally induced drift in the relative phase is corrected every few minutes using a liquid crystal (LC) phase retarder. The MZ is polarization based in a collinear inherently phase stable design. The MZ phase is controlled using an additional LC phase retarder at 45 degrees ( $X, Y$  pol.). The spatial and spectral modes are matched using a polarization maintaining fiber (PMF) and a 3nm FWHM band-pass filter (BPF). Photon number resolving detection is performed using an array of single photon counting modules (SPCM, Perkin Elmer).

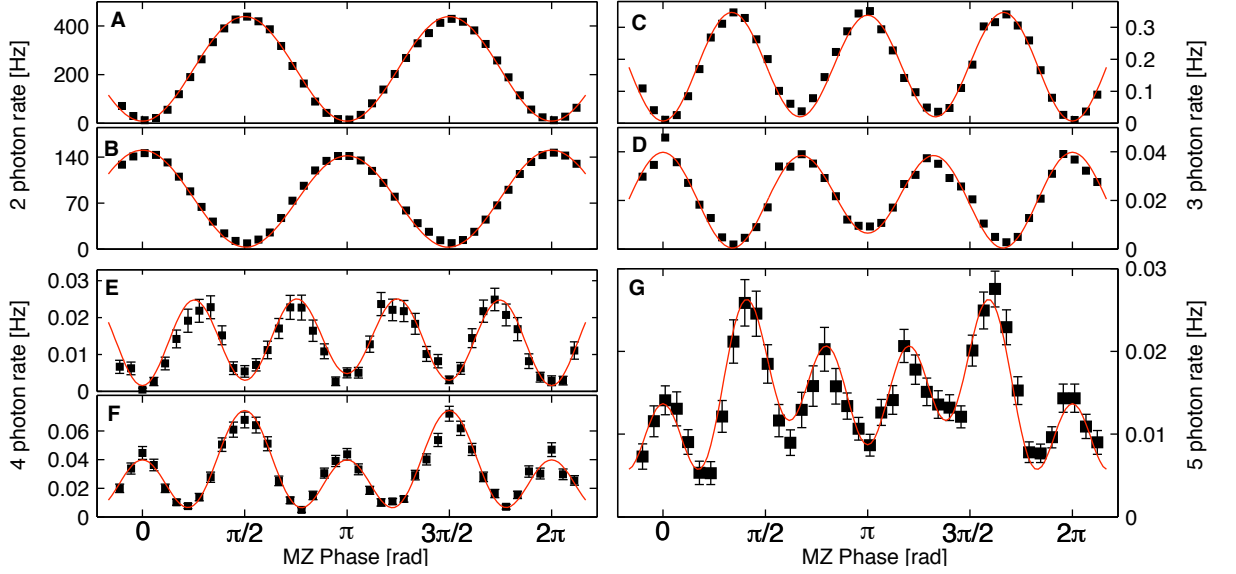


Figure 3: Experimental results. Coincidence measurements demonstrating  $N$ -fold super-resolution for  $N = 2, 3, 4$  and  $5$  with no background subtraction. Error bars indicate  $\pm\sigma$  statistical uncertainty. The number of 'clicks' in detector  $D_{1,(2)}$  is denoted  $N_{1,(2)}$  (see Fig. 1). Two photon rate with **A**,  $N_1, N_2 = 1, 1$  and **B**,  $N_1, N_2 = 0, 2$ . Three photon rate with **C**,  $N_1, N_2 = 2, 1$  and **D**,  $N_1, N_2 = 0, 3$ . Four photon rate with **E**,  $N_1, N_2 = 3, 1$  and **F**,  $N_1, N_2 = 2, 2$ . Five photon rate with **G**,  $N_1, N_2 = 2, 3$ . Solid lines are obtained using an analytical model (see supporting online text). For each  $N$  the pair amplitude ratio  $\gamma$ , was chosen separately to maximize the NOON state fidelity. The optimal values (obtained analytically) are  $\gamma_2 = \gamma_3 = 1$ ,  $\gamma_4 = \sqrt{3}$  and  $\gamma_5 = 9/(\sqrt{10} + 1) \approx 2.16$ . Visibility of the sinusoidal patterns with  $N$  oscillations is determined by a weighted least squares sin, cos decomposition restricted to frequencies of  $0, 1, \dots, N$ . The values for plots **A** - **G** are  $V = (95 \pm 0.0)\%$ ,  $(88 \pm 0.03)\%$ ,  $(86 \pm 0.6)\%$ ,  $(80 \pm 1.9)\%$ ,  $(74 \pm 3)\%$ ,  $(73 \pm 2.4)\%$  and  $(42 \pm 2)\%$  respectively.

# Supporting Online Material– Realization of High-NOON States by Mixing Quantum and Classical Light

Itai Afek, Oron Ambar, Yaron Silberberg\*

Department of Physics of Complex Systems, Weizmann Institute of Science,  
Rehovot 76100, Israel

\* E-mail: yaron.silberberg@weizmann.ac.il

These supporting online materials contain a complete theoretical analysis of our experiment. In Sec. 1 we develop the analytical model used for calculating the theoretical curves in Fig. 3 of the main text. A brief discussion of the overall setup transmission and its importance is given in Sec. 2. In Sec. 3 we illustrate the feasibility of nine-photon NOON state generation in our setup using the theoretical model.

## 1 Analytical Model

The experimental results in Fig. 3 of the main text contain multiphoton coincidence rates as a function of the Mach-Zehnder (MZ) phase  $\varphi$ . The probability for detecting  $n_1$  photons in  $D_1$  and  $n_2$  photons in  $D_2$  simultaneously (see experimental setup in Fig. 2 of the main text) is given by (1)

$$p_{n_1, n_2}(\varphi) = \text{Tr} \left[ \hat{U}(\varphi) |\alpha\rangle\langle\alpha|_a \otimes |\xi\rangle\langle\xi|_b \hat{U}^\dagger(\varphi) \hat{\pi}_{n_1}^1 \otimes \hat{\pi}_{n_2}^2 \right], \quad (1)$$

where  $\hat{U}(\varphi)$  is a unitary operator describing the MZ using angular momentum notation (2)

$$\hat{U}(\varphi) = e^{i(\pi/2)\hat{J}_x} e^{-i\varphi\hat{J}_z} e^{-i(\pi/2)\hat{J}_x}. \quad (2)$$

The coherent and down-conversion input states  $|\alpha\rangle, |\xi\rangle$  are defined the in the conventional way,

$$|\alpha\rangle = \sum_{n=0}^{\infty} e^{-\frac{1}{2}|\alpha|^2} \frac{\alpha^n}{\sqrt{n!}} |n\rangle, \quad \alpha = |\alpha|e^{i\phi_{cs}}$$

$$|\xi\rangle = \frac{1}{\sqrt{\cosh r}} \sum_{m=0}^{\infty} (-1)^m \frac{\sqrt{(2m)!}}{2^m m!} (\tanh r)^m |2m\rangle, \quad (3)$$

and  $\hat{\pi}_n^{1(2)}$  are the positive-operator-valued measures (POVM) (3) of detectors  $D_{1(2)}$  defined,

$$\hat{\pi}_n^{1(2)} = \sum_{k=0}^{\infty} \theta_k^{(n)} |k\rangle\langle k|_{1(2)}, \quad \theta_k^{(n)} = [C_{2(3)} \cdot L(\eta)]_{n,k}. \quad (4)$$

The POVM introduces experimental imperfections via two matrices,  $C_N$  and  $L(\eta)$ . The abstract loss model (4) allows us to account for all the sources of loss in the experiment using a single parameter  $\eta$  representing the overall transmission. The non-zero loss matrix elements are given by

$$[L(\eta)]_{n,m} = \binom{m-1}{n-1} \eta^{n-1} (1-\eta)^{m-n} \quad n, m = 1, 2, \dots \quad (5)$$

Each of our photon number resolving detectors consists of two ( $D_1$ ) or three ( $D_2$ ) avalanche photodiodes (APD) such that the incoming photons are distributed equally between them. This construction is reflected in the POVM via the matrix  $C_N$ , where  $N$  represents the number of sub-detectors. The matrix elements of  $C_N$  for  $N = 2, 3$  are given by

$$[C_2]_{1,1} = 1;$$

$$\begin{cases} [C_2]_{2,k} = \frac{1}{2^{k-2}}; \\ [C_2]_{3,k} = 1 - [C_2]_{2,k}; \end{cases} \quad k = 2, 3, \dots \quad (6)$$

$$\begin{aligned}
& [C_3]_{1,1} = 1; \\
& [C_3]_{2,2} = 1; \\
& \begin{cases} [C_3]_{2,k} = \frac{1}{3^{k-2}}; \\ [C_3]_{3,k} = 1 - \frac{1}{3^{k-2}} \times (2^{k-1}); \\ [C_3]_{4,k} = 1 - [C_3]_{2,k} - [C_3]_{3,k}; \end{cases} \quad k = 3, 4 \dots
\end{aligned} \tag{7}$$

Finally, to obtain the measured count rate, the probability of Eq.(1) should be multiplied by the repetition rate of 80 MHz.

## 2 Overall Transmission

The overall transmission  $\eta$  is an important experimental factor which determines the obtainable visibility of super-resolution. In our setup, we find  $\eta = 0.12$  by inserting down-conversion only and measuring the coincidence to singles ratio. Roughly, this transmission has three multiplicative contributions  $\eta \sim \eta_1 \times \eta_2 \times \eta_3$ . The first contribution  $\eta_1 \sim 0.5$  results from the fiber pair-coupling ratio. The band-pass filter induces an additional effective loss,  $\eta_2 \sim 0.5$ , and finally the detector efficiencies together with various coating imperfections contribute  $\eta_3 \sim 0.5$ .

Most of the photons originate in our experiment originate from the coherent (classical) light source which is practically unlimited in intensity. In fact, it can be shown that  $\gamma_N \sim N/2$  for large  $N$  where  $\gamma_N$  is the optimal pair amplitude ratio for a given photon number  $N$ . Thus, the coherent state's two photon probability is approximately  $N^2/4$  times higher than that of the SPDC i.e. the higher the value of  $N$  the larger the ratio of classical to quantum resources. Therefore, measuring larger states does not require a brighter SPDC source. Thus, the only limiting factor is the overall transmission,  $\eta$ . Simulations show that using an overall transmission of  $\eta = 0.5$ , nine photon entanglement is readily observable even with the current, relatively modest, SPDC flux. In this respect, our experiment highlights the need for high purity SPDC

sources which can be spectrally mode matched to a coherent state. Improved transmission can be obtained by way of SPDC generation in separable spectral modes (5–7) allowing removal of the 3nm band-pass filter. In addition, improved single mode coupling of the photon pairs and use of high efficiency photon number resolving detectors (8, 9) are instrumental.

### 3 Nine Photon NOON State

In this section we show that our setup is capable of generating nine photon NOON states when using a reasonable overall transmission  $\eta = 0.5$ . This transmission could be obtained by using improved photon number resolving detectors, improved pair coupling to the fiber and using down-conversion which is separable in frequency modes. The analytical model of Sec. 1 allows us to investigate the behavior of our setup using any chosen overall transmission  $\eta$ . We note that for  $N = 9$ , the pair amplitude ratio is  $\gamma_9 = 3.9$  implying that the coherent light photon-pair probability is  $(\gamma_9^2 =) 15.3$  times higher than for the down-conversion. In supplementary Fig. 1 we show the nine-photon coincidence rate employing our existing down-conversion flux, using  $\eta = 1$  (Fig. 1A) and  $\eta = 0.5$  (Fig. 1B). This illustrates that our setup allows measurement of nine photon super-resolution originating from NOON states when using a feasible transmission.

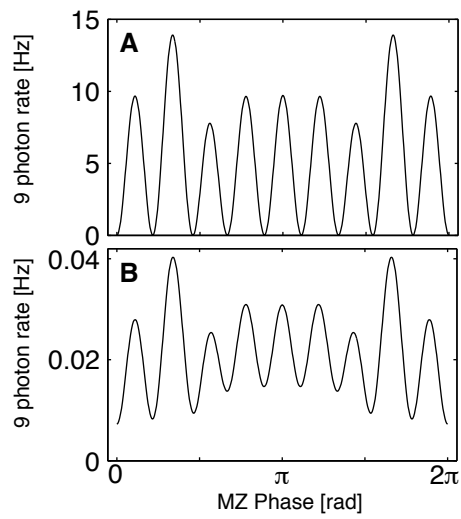


Figure 1: Simulation of nine-photon coincidence rates using two different overall transmission values. Nine-fold coincidence rates vs. MZ phase. For this measurement  $N_1 = 6, N_2 = 3$ . **A** using  $\eta = 1$ , **B** using  $\eta = 0.5$ .

## References

1. K. L. Pregnell, D. T. Pegg, *Phys. Rev. A* **66**, 013810 (2002).
2. B. Yurke, S. L. McCall, J. R. Klauder, *Phys. Rev. A* **33**, 4033 (1986).
3. J. S. Lundeen, *et al.*, *Nat. Phys.* **5**, 27 (2009).
4. D. Achilles, *et al.*, *J. Mod. Opt.* **51**, 1499 (2004).
5. P. J. Mosley, *et al.*, *Phys. Rev. Lett.* **100**, 133601 (2008).
6. P. J. Mosley, J. S. Lundeen, B. J. Smith, I. A. Walmsley, *New. J. Phys.* **10**, 093011 (2008).
7. A. Valencia, A. Ceré, X. Shi, G. Molina-Terriza, J. P. Torres, *Phys. Rev. Lett.* **99**, 243601 (2007).
8. C. Silberhorn, *Contemp. Phys.* **48**, 143.
9. A. E. Lita, A. J. Miller, S. W. Nam, *Opt. Express* **16**, 3032 (2008).